Many-Body Chaos in Thermalized Fluids

Sugan Durai Murugan,[1,*] Dheeraj Kumar,[2,1,†] Subhro Bhattacharjee,[1,‡] and Samriddhi Sankar Ray[1,§]
[1]International Centre for Theoretical Sciences, Tata Institute of Fundamental Research, Bengaluru 560089, India
[2]PMMH, CNRS, ESPCI Paris, Université PSL, Sorbonne Université, Université de Paris, 75005 Paris, France

(Received 25 May 2021; accepted 15 August 2021; published 15 September 2021)

Linking thermodynamic variables like temperature T and the measure of chaos, the Lyapunov exponents λ, is a question of fundamental importance in many-body systems. By using nonlinear fluid equations in one and three dimensions, we show that in thermalized flows $\lambda \propto \sqrt{T}$, in agreement with results from frustrated spin systems. This suggests an underlying universality and provides evidence for recent conjectures on the thermal scaling of λ. We also reconcile seemingly disparate effects—equilibration on one hand and pushing systems out of equilibrium on the other—of many-body chaos by relating λ to T through the dynamical structures of the flow.

DOI: 10.1103/PhysRevLett.127.124501

Many-body chaos is the key mechanism to explain the fundamental basis—*thermalization* and *equilibration*—of statistical physics. However, there are equally important examples in nature, such as turbulence, where chaos plays a role that is seemingly *opposite* from the *settling down* through thermalization and equilibration of several many-body systems. This contrast becomes stark if we argue in terms of the celebrated *butterfly effect* [1–4]: while the amplification of the *wingbeat* results in complex dynamical macroscopic structures in driven-dissipative systems (e.g., a turbulent fluid), the same amplification leads to a loss of memory of initial conditions, resulting in ergodic behavior and eventual thermalization or equilibration, in Hamiltonian many-body systems. How then do we reconcile these two apparently disparate roles of many-body chaos?

An important piece of the answer lies in investigating the spatiotemporal aspects (the Lyapunov exponent λ and butterfly speed v_B) of many-body chaos in fluids to reveal its connection with macroscopic (thermodynamic) characterization of the system. This provides for comparisons of length scales and timescales of chaos and thermalization, on the one hand, and the nonlinear dynamic structures of the fluid-velocity field on the other.

Characterizations of chaos and its connection with transport and hydrodynamics are recent in the context of both classical and quantum many-body systems like unfrustrated and frustrated [5–8] magnets, strongly correlated field theories [9–17], and field theories of black holes [18,19]. A common feature responsible for the unconventional signatures of chaos in many of these systems seems to originate from a large set of strongly coupled, dynamic, low energy modes arising from competing interactions. This is similar a turbulent fluid where the triadic interactions of velocity (Fourier) modes across several decades lead to strong couplings resulting in, e.g., scale-by-scale energy transfers [20,21].

These studies have been facilitated by the development of quantum *out-of-time commutators* (OTOCs) [5,16,22–26] and their classical counterpart the *decorrelator* [5,6] which measure how two *very* nearly identical copies of a system decorrelate spatiotemporally. The classical decorrelators are invaluable for understanding the butterfly effect [1–4] in nonintegrable, chaotic, classical many-body systems through the measurement of λ and v_B. Since by construction, these OTOCs or decorrelators provide a unified framework to bridge thermodynamic variables (e.g., temperature T) with the butterfly effect, they are a unique prescription to connect many-body chaos with the foundations of statistical approaches in *both* classical and quantum many-body systems. The most striking example of this is that while for quantum systems, $\lambda \leq T/\hbar$, limiting the rate of scrambling [23], the analogous *conjecture* for classical systems is $\lambda \propto \sqrt{T}$ at low temperatures [23,27].

In this Letter, by using a model of *thermalized fluids*, we derive $\lambda \propto \sqrt{T}$ and demonstrate a possible universality of many-body chaos without an apparent (weakly interacting) quasiparticle description, and hence a kinetic theory. Interestingly, we show how decorrelators *sense* the emergent dynamical structures of the fluid-velocity field, providing an elegant way to bridge the ideas of many-body chaos with foundational principles of statistical physics: thermalization, equilibration, and ergodicity.

For classical systems, recent understanding of spatiotemporal chaos through decorrelators stems primarily from spin systems [6–8]. However, these ideas have not been applied for the most ubiquitous of chaotic, nonlinear, systems: turbulent flows. This is because, unlike spin systems, turbulent flows, governed by the viscous Navier-Stokes equation, are an example of a driven-dissipative

system *without* a Hamiltonian or a statistical physics description in terms of thermodynamic variables. Therefore, we look for variations of the Navier-Stokes equation which, while preserving the same nonlinearity, nevertheless has a Hamiltonian structure, resulting in a chaotic, thermalized fluid.

Such a prescription leads to the inviscid, three-dimensional (3D) Euler and one-dimensional (1D) Burgers equations, but retaining only a finite number of Fourier modes through a (Fourier) Galerkin truncation [28–31]. Such a projection of the partial differential equations onto a finite-dimensional subspace ensures conservation of momentum, energy, and phase space, *and* guarantees chaotic solutions for the flow field which thermalizes. These thermalized fluids (see Supplemental Material [32]) are characterized by energy equipartition and velocity fields with Gibbs distribution $\mathcal{P}[\mathbf{v}]d\mathbf{v} = (3/2\pi E)^{3/2}\exp[-3\mathbf{v}^2/2E]d\mathbf{v}$ as illustrated in Fig. 1. Here, E is the conserved energy density of the system satisfying $\langle \frac{1}{2}\mathbf{v}^2\rangle = E$. This allows us to define a *temperature*, $T = \frac{2}{3}E$ such that the different thermalized configurations describe a canonical ensemble. A thermalized fluid is thus not dissimilar to that of correlated many-body condensed matter systems (e.g., frustrated magnets) where the microscopic memory does not dictate the dynamical correlations.

These thermalized fluids set the platform for addressing the primary question of the growth of perturbations in a classical, chaotic system. To do this, in the 3D Euler, an arbitrary realization of the thermalized solution $\mathbf{v}_0^{\mathbf{a}} = \mathbf{v}^{\text{th}}$ is taken and a second copy generated, with a perturbation in velocity field, $\mathbf{v}_0^{\mathbf{b}} = \mathbf{v}_0^{\mathbf{a}} + \boldsymbol{\delta}\mathbf{v}_0$. Here, $\boldsymbol{\delta}\mathbf{v}_0 = \boldsymbol{\nabla}\times\mathbf{A}$, with $A_i = \epsilon\sqrt{E}r_0\exp[-(r^2/2r_0^2)]\hat{e}_i$, is an infinitesimal (characterized by $\epsilon \ll 1$) perturbation centered at the origin and which falls off rapidly with distance r (with the reference scale $r_0 \ll 2\pi$) making it *spatially localized*.

We now evolve [32] the Galerkin-truncated Euler equation, *independently* for the two copies, with initial conditions $\mathbf{v}_0^{\mathbf{a}}$ and $\mathbf{v}_0^{\mathbf{b}}$ to obtain (thermalized) solutions $\mathbf{v}^{\mathbf{a}}(\mathbf{x},t)$ and $\mathbf{v}^{\mathbf{b}}(\mathbf{x},t)$ and thence the *difference field* $\boldsymbol{\delta}\mathbf{v}(\mathbf{x},t) = \mathbf{v}^{\mathbf{b}}(\mathbf{x},t) - \mathbf{v}^{\mathbf{a}}(\mathbf{x},t)$. Since initially this difference field $\boldsymbol{\delta}\mathbf{v}(\mathbf{x},0) \equiv \boldsymbol{\delta}\mathbf{v}_0$ was spatially localized and vanishingly small, its subsequent spatiotemporal evolution reflects how the butterfly effect manifests itself in such systems. Fundamentally, this is a question of how systems **a** and **b** decorrelate and intimately connected with questions of ergodicity and thermalization.

To make this assessment rigorous, we construct the spatially resolved decorrelator $\phi(\mathbf{x},t) = \langle \frac{1}{2}|\boldsymbol{\delta}\mathbf{v}(\mathbf{x},t)|^2\rangle$, where $\langle\cdots\rangle$ denotes averaging over configurations taken from the thermalized ensemble and distance is measured from origin where the perturbation is seeded at $t = 0$. In Fig. 2 (see movie in Supplemental Material [32] for the full evolution) we show the spatial profile (in the $z = 0$ plane) of $|\boldsymbol{\delta}\mathbf{v}(\mathbf{x},t)|^2$ for a particular initial realization of systems **a** and **b** at two different instants of time. While at very early times $t = 0^+$, panel (a), $|\boldsymbol{\delta}\mathbf{v}(\mathbf{x},t)|^2$ remains small but diffuses *instantly* and *arbitrarily*, a more striking behavior is seen at later times [panel (b)] when the spatial spread is controlled by the strain in the velocity field as we shall see below. [It is likely that the initial, instantaneous spread is a result of the nonlocality (in space) of the 3D fluid because of the pressure term; however, since the Galerkin truncation also introduces an additional nonlocality, the precise mechanism for the initial spread is hard to pin down.]

Since the thermalized fluid is *statistically* isotropic, the decorrelator $\phi(\mathbf{x},t)$ is a function of $|\mathbf{x}|$. We exploit this to construct the more tractable angular-averaged decorrelator $\phi(r,t) = (1/4\pi r^2)\int d\boldsymbol{\Omega}_r\phi(\mathbf{x},t)$.

Given the nonlocality of the 3D Euler equation, these systems differ crucially from spin systems in the absence of pilot waves and a distinct velocity scale akin to a butterfly speed [5,6]. Instead, decorrelators for 3D thermalized fluids have a self-similar spatial profile $\phi(r,t) \sim r^{-\alpha}$ (with $\alpha \sim 4$). The lack of a sharp wave front and self-similarity is evident

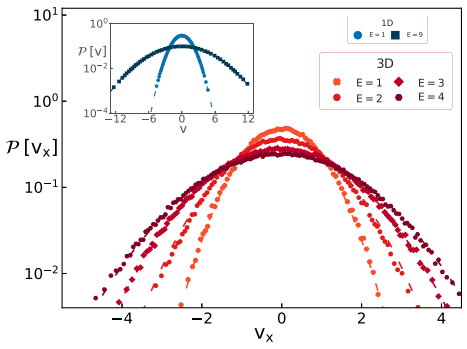

FIG. 1. Probability distribution functions of the x component of the thermalized velocity field from Galerkin-truncated 3D Euler and (inset) 1D Burgers simulations for different energies; dashed lines denote the corresponding Gibbs distribution.

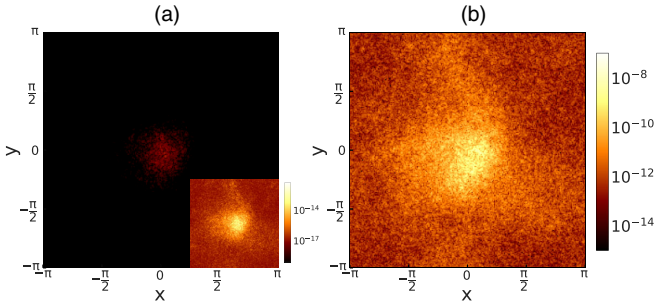

FIG. 2. Representative plots of the difference field $|\boldsymbol{\delta}\mathbf{v}(\mathbf{x},t)|^2$, along the $z = 0$ plane of a 3D thermalized fluid (with energy $E = 2.0$ and a perturbation amplitude $\epsilon = 10^{-6}$ at (a) early ($t = 0.4$) and (b) later (0.7) times. The inset of panel (a) shows the same early time data, with a magnified scale, to reveal a somewhat *self-similar* spatial structure that arises from nonlocal interactions (see main text and movie in Supplemental Material [32]).

from Fig. 2(b) and the inset of Fig. 2(a). Therefore, to track the temporal evolution of the decorrelator it is convenient to introduce the space-averaged decorrelator $\Phi(t) = (1/V)\int d^3\mathbf{x}\phi(\mathbf{x},t)$ which then serves as a diagnostic for the temporal aspects of this problem.

This allows us, starting from the 3D Euler equation, to derive the evolution equation

$$\dot{\Phi}(t) = -\overline{\langle \delta v_i S_{ij} \delta v_j \rangle} \tag{1}$$

in terms of the familiar rate-of-strain tensor $2S_{ij} = \partial_i v_j^{\mathrm{a}} + \partial_j v_i^{\mathrm{a}}$; the overbar in the definition denotes a spatial average.

By using the eigenbasis of $\mathbf{S}$, we rewrite the above equation as $\dot{\Phi} = -\sum_{i=1}^{3} \overline{\langle \hat{\alpha}_i^2 \gamma_i |\boldsymbol{\delta}\mathbf{v}|^2 \rangle}$ where $\{\gamma_i\}$ are the three eigenvalues and $\{\hat{\alpha}_i\}$ are the direction cosines of $\boldsymbol{\delta}\mathbf{v}$ along the three eigendirections. Equation (1), which formally resembles the enstrophy production term for the Euler equation [39,40], is an important result that *connects* the decorrelator with the dynamical structures of the velocity field.

Our direct numerical simulations (DNSs) [32] of the truncated 3D Euler equation show strong evidence that the difference fields preferentially grow, at *short* times, along the compressional eigendirection ($i = 3$) of the thermalized fluid leading to a further simplification $\dot{\Phi} \approx -\overline{\langle \hat{\alpha}_3^2 \gamma_3 |\boldsymbol{\delta}\mathbf{v}|^2 \rangle}$. Since by definition $\gamma_3 < 0$, this ensures not only the positive definiteness of $\dot{\Phi}(t)$, but also, since (up to constants) $\dot{\Phi}(t) \sim -\bar{\gamma}_3 \Phi$, an exponential growth with a Lyapunov exponent $\lambda \sim |\bar{\gamma}_3|$ at short times (Fig. 5). This connects the straining of the flow field with λ.

How robust is this *short-time* behavior with respect to both dimension and the compressibility of the flow?

The answer lies in an analysis of the 1D (compressible) Burgers equation with N_G Fourier modes. Furthermore, to underline the universality of our results, this time we construct the decorrelator and carry out the theoretical [32] and numerical analysis entirely in Fourier space. As before, from the thermalized solution (in Fourier space) $\hat{v}^{\mathrm{th}}$, defining a control field $\hat{v}_0^{\mathbf{a}} = \hat{v}^{\mathrm{th}}$ and a perturbed field $\hat{v}_0^{\mathbf{b}} = \hat{v}_0^{\mathbf{a}}(1 + \epsilon\delta_{k,k_p})$ with large values of the perturbation wave number k_p to generate delocalized small-scale perturbations in the systems [32]. It is important to stress that given the seed perturbation is localized in Fourier space in 1D (and hence delocalized in physical space), the spatial spread of perturbations, which is relevant and studied for 3D fluids in this Letter, remains outside the scope of analysis here.

As before, both systems are evolved independently and the Fourier space decorrelator $|\hat{\Delta}_k|^2 = \langle |\hat{v}_k^{\mathbf{a}} - \hat{v}_k^{\mathbf{b}}|^2 \rangle$, measured, mode by mode, as a function of time. Given the relative analytical simplicity of the 1D system, we construct the equation of motion of $|\hat{\Delta}_k|^2$ and derive an exponential growth of the decorrelator associated with a Lyapunov exponent λ. Thus, the theoretical calculations for the 1D model are not only consistent with the more complex 3D system but also provide, as we see below, a more rigorous insight into how the Lyapunov exponent scales with T and the degrees of freedom N_G of our system. (See Supplemental Material [32] for the derivation of the linear theories describing the short-time dynamics of the decorrelator.)

At long times, since systems **a** and **b** decorrelate $\langle \mathbf{v}^{\mathbf{a}} \cdot \mathbf{v}^{\mathbf{b}} \rangle = 0$, leading to a suspension of the underlying approximations in the linear theory presented above, Φ and $|\hat{\Delta}_k|^2$ must saturate to a value equal to $2E$ and $2E/N_G$, respectively.

With these theoretical insights for both the 1D and 3D systems, we test them against results from our numerical simulations. In Fig. 3 we show representative results for $\phi(r,t)$ (Φ in the upper inset) from 3D Euler and $|\hat{\Delta}_k|^2$ for the 1D Burgers (lower inset) versus time on a semilog scale. The symbols (for different values of r and k) are results from the full nonlinear DNSs while the dashed lines correspond to decorrelators obtained from the linearized theory.

Consistent with our theoretical estimates described above, the decorrelators from the full, nonlinear DNSs (shown by symbols) grow exponentially (positive λ) before eventually saturating (as the two systems decorrelate) to a value set by the energy. The agreement between these decorrelators and the ones we estimate theoretically through a linearized model (dashed lines) is remarkable during the early time exponential phase. However, decorrelators constructed from the linearized model (valid for short times) are insensitive to nonlinearities and continue growing exponentially, while the ones from the full

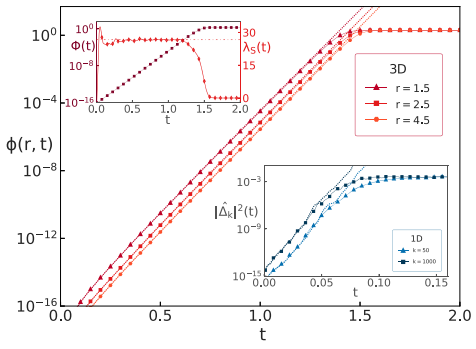

FIG. 3. Semilog plots of $\phi(r,t)$ ($E = 1.0$) and (lower inset) $|\hat{\Delta}_k|^2$ ($E = 2.0$) showing an initial exponential growth and eventual saturation. The dashed lines, from linearized theory, are in excellent agreement with DNSs at early times. Upper inset: semilog (left y axis) plot of $\Phi(t)$ (3D fluid) along with results from our linearized theory (dashed line). λ, extracted from $\Phi(t)$, shown as dash-dotted horizontal line, agrees well with λ_S (linearized theory, right y axis).

nonlinear system eventually saturate. We will soon return to the question of timescales which determine this saturation.

Finally, we confirm the validity of Eq. (1) by showing (upper inset, Fig. 3) the agreement between $\lambda_S(t) = -\overline{\langle \delta v_i S_{ij} \delta v_j \rangle}/\Phi(t)$ and the Lyapunov exponent λ extracted from the decorrelator $\Phi(t)$ measured in DNSs. The agreement between the two is almost perfect at short times before $\lambda_S(t)$ decays to zero as the decorrelator saturates.

This inevitably leads us to the central question of this work: how fast do perturbations grow in a classical, chaotic system and how does it depend on the temperature T as well as the number of modes, N_G? Furthermore, is the scaling behavior of λ really universal?

Although nonlinear equations for hydrodynamics do not yield easily to an analytical treatment, it is tempting to theoretically estimate the functional dependence of λ on T and N_G. An extensive analysis [32] of the linearized equations for $\Phi(t)$ and $|\hat{\Delta}_k|^2$ show that under very reasonable approximations, which were tested against data, $\lambda \propto N_G\sqrt{T}$. Whereas for the Euler fluid this scaling is a consequence of the statistics of the strain-rate tensor which determines the behavior of $\Phi(t)$, the analogous result for the 1D system is obtained by straightforward algebraic manipulations, factoring in the statistical fluctuations, of the equation governing the evolution of $|\hat{\Delta}_k|^2$.

Our theoretical prediction is easily tested by measuring λ in DNSs of the full nonlinear 3D Euler and 1D Burgers equations. From plots such as in Fig. 3, we extract the mean λ and its (statistical) error bar, and examine its dependence on temperature T (and N_G) by changing the magnitude of the initial conditions and hence the initial energy or temperature. (Surprisingly, λ measured through such decorrelators are independent of r or k, as was already suggested in Fig. 3.) Figure 4 shows a unified (3D Euler and 1D Burgers) log-log plot of all the rescaled Lyapunov exponent λ/N_G measured—for different strengths and scales of perturbations and N_G—as a function of temperature T.

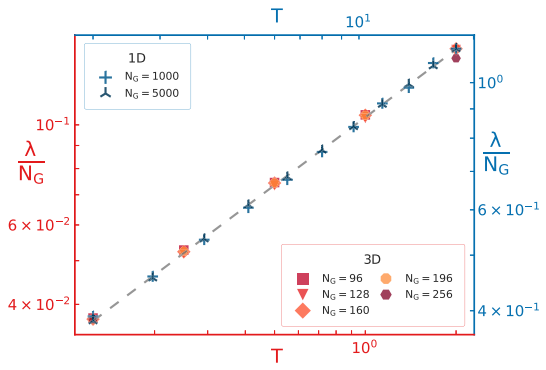

FIG. 4. Log-log plot of λ/N_G versus T for the 3D (axes in red) and 1D (axes in blue) thermalized fluids corresponding to different values of ϵ, N_G, and, for the 1D fluid, k_p. The dashed line $\propto \sqrt{T}$ confirms our theoretical prediction.

The collapse of the data on the dashed line, denoting a $\sqrt{T}$ scaling, shows that the many-body chaos of such thermalized fluids *is* characterized by the behavior $\lambda \propto N_G\sqrt{T}$. It is worth stressing that these DNS results for the 3D Euler equations make the theoretical bound [32] sharp.

These, to the best of our knowledge, are the first results, and confirmation of earlier conjectures [23,27] and demonstrations for classical spin systems [6], that $\lambda \propto \sqrt{T}$ in a chaotic and nonlinear, many-body classical system obeying the equations of hydrodynamics. Remarkably, we also find strong evidence that λ scales linearly with N_G in such extended systems and independent of spatial dimension and compressibility of the flow.

Given the association of many-body chaos with ergodicity and equilibration in classical statistical physics, how well do measurements of λ relate to the (inverse) timescales associated with the loss of *memory*? The simplest measure of how fast a system *forgets* is the ensemble-averaged autocorrelation function $C(t) = (2E)^{-1}\langle \mathbf{v}^{\rm th}(t) \cdot \mathbf{v}^{\rm th}(0)\rangle$ (Fig. 5). It is easy to show [32] that $C(t) \approxeq \exp[-(t^2/2\tau^2)]$ with an autocorrelation time $\tau \sim 1/\lambda$ as clearly shown from our measurements (upper inset, Fig. 5). This association of τ with λ provides a firm foundation to interpret the salient features of many-body chaos in terms of principles of statistical physics: ergodicity and thermalization. A further connection is established through the relation between the timescales $t_{\rm sat} \sim \tau \sim 1/\lambda$ at which the decorrelator saturates as $\Phi(t) \approxeq 2E(1 + \exp[-\lambda(t - t_{\rm sat})])^{-1}$.

The generality of the OTOCs and cross-correlators lead to questions of connecting the macroscopic variables with the scales of chaos in the most canonical of chaotic systems: those described by nonlinear equations of hydrodynamics. Here, we provide the first evidence of the temperature dependence of the Lyapunov exponent in (continuum) classical nonlinear hydrodynamic systems and show its robustness with respect to spatial dimensions and compressibility effects. It is important to underline that

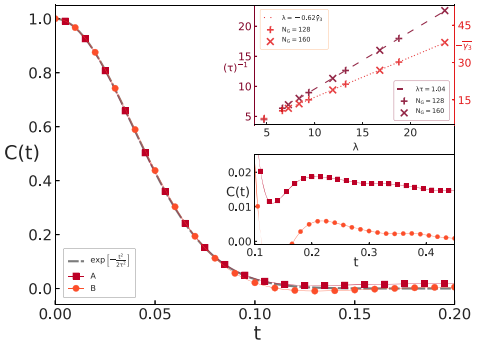

FIG. 5. A plot of $C(t)$ for a (a) *nearly* and (b) *completely* thermalized 3D fluid along with the theoretical Gaussian prediction. Lower inset: a magnified view shows that for a fluid which is not completely thermalized, $C(t)$ falls off to zero much more slowly. Upper inset: representative plots of τ and the average (negative) eigenvalue (compressional direction) versus λ.

many-body chaos and $\lambda \sim N_G\sqrt{T}$ is really an emergent feature of a fluid which is thermalized. We checked this explicitly by measuring the decorrelators in the flow *before* it thermalizes and found, despite the conservation laws still holding, no associated exponential growth and spread of the difference field. Furthermore, our measured λ should be identified with the largest Lyapunov exponent of the system and that $t_{\rm sat}$ is a useful estimate of thermalization (or equilibration) time.

Finally, the temperature dependence of λ is consistent with recent results for classical spin liquids without quasiparticles [6–8,41] as well as more general dimensional arguments based on phase-space dynamics [27] of classical many-body systems. In this regard we note that in classical spin systems [7], the existence of low energy quasiparticles seems to *reduce* the chaotic behavior of the system ($\lambda \propto T^a$, $a > 0.5$). While more detailed and theoretical investigation of these features, as well as, how far they are relevant for the spontaneously stochastic Navier-Stokes turbulence are interesting future directions, this butterfly effect for classical, nonlinear, hydrodynamic systems seems to be robust and generic.

While it is probably true that the exact nature of the dependence of the Lyapunov exponent on the temperature (or energy density) and number of degrees of freedom should vary from system to system, the evidence we provide of their interdependence opens new avenues and questions. In particular, these studies demonstrate the dependence of signatures of spatiotemporal chaos on the thermodynamic variables as well its relation with the transport properties.

We thank S. Banerjee, J. Bec, M. E. Brachet, A. Dhar, A. Kundu, A. Das, S. Chakraborty, T. Bilitewski, R. Moessner, and V. Shukla for insightful discussions. The simulations were performed on the ICTS clusters *Mowgli*, *Mario*, *Tetris*, and *Contra* as well as the work stations from Project No. ECR/2015/000361: *Goopy* and *Bagha*. D. K. and S. S. R. acknowledges DST (India) project DST (India) Project No. MTR/2019/001553 for financial support. S. B. acknowledges MPG for funding through the Max Planck Partner group on strongly correlated systems at ICTS. D. K. and S. B. acknowledge SERB-DST (India) for funding through project Grant No. ECR/2017/000504. This research was supported in part by the International Centre for Theoretical Sciences (ICTS) for the online program - Turbulence: Problems at the Interface of Mathematics and Physics (code: ICTS/TPIMP2020/12). The authors acknowledges the support of the DAE, Government of India, under Project No. 12-R&D-TFR-5.10-1100 and Project No. RTI4001.

*sugan.murugan@icts.res.in
†dheeraj.kumar@espci.fr
‡subhro@icts.res.in
§samriddhisankarray@gmail.com

[1] E. N. Lorenz, J. Atmos. Sci. **20**, 130 (1963).
[2] E. N. Lorenz, *The Essence of Chaos* (University of Washington Press, Seattle, Washington, 1993), https://nla.gov.au/nla.cat-vn107980.
[3] E. Lorenz, in The Chaos Avant-Garde (World Scientific, Singapore, 2000), https://www.worldscientific.com/doi/abs/10.1142/9789812386472_0007.
[4] R. C. Hilborn, Am. J. Phys. **72**, 425 (2004).
[5] A. Das, S. Chakrabarty, A. Dhar, A. Kundu, D. A. Huse, R. Moessner, S. S. Ray, and S. Bhattacharjee, Phys. Rev. Lett. **121**, 024101 (2018).
[6] T. Bilitewski, S. Bhattacharjee, and R. Moessner, Phys. Rev. Lett. **121**, 250602 (2018).
[7] T. Bilitewski, S. Bhattacharjee, and R. Moessner, Phys. Rev. B **103**, 174302 (2021).
[8] S. Ruidas and S. Banerjee, arXiv:2007.12708.
[9] M. Blake, Phys. Rev. Lett. **117**, 091601 (2016).
[10] M. Blake, R. A. Davison, and S. Sachdev, Phys. Rev. D **96**, 106008 (2017).
[11] Y. Gu, A. Lucas, and X.-L. Qi, SciPost Phys. **2**, 018 (2017).
[12] A. Lucas, arXiv:1710.01005.
[13] Y. Werman, S. A. Kivelson, and E. Berg, arXiv:1705.07895.
[14] A. A. Patel, D. Chowdhury, S. Sachdev, and B. Swingle, Phys. Rev. X **7**, 031047 (2017).
[15] A. A. Patel and S. Sachdev, Proc. Natl. Acad. Sci. U.S.A. **114**, 1844 (2017).
[16] A. Y. Kitaev, KITP Program: Entanglement in Strongly-Correlated Quantum Matter (Kavli Institute for Theoretical Physics, 2015).
[17] S. Banerjee and E. Altman, Phys. Rev. B **95**, 134302 (2017).
[18] S. H. Shenker and D. Stanford, J. High Energy Phys. 03 (2014) 067.
[19] J. S. Cotler, G. Gur-Ari, M. Hanada, J. Polchinski, P. Saad, S. H. Shenker, D. Stanford, A. Streicher, and M. Tezuka, J. High Energy Phys. 05 (2017) 118.
[20] R. H. Kraichnan, J. Fluid Mech. **47**, 525 (1971).
[21] S. A. Orszag, J. Fluid Mech. **41**, 363 (1970).
[22] A. I. Larkin and Y. N. Ovchinnikov, Sov. J. Exp. Theor. Phys. **28**, 1200 (1969).
[23] J. Maldacena, S. H. Shenker, and D. Stanford, J. High Energy Phys. 08 (2016) 106.
[24] D. A. Roberts and D. Stanford, Phys. Rev. Lett. **115**, 131603 (2015).
[25] B. Dóra and R. Moessner, Phys. Rev. Lett. **119**, 026802 (2017).
[26] I. L. Aleiner, L. Faoro, and L. B. Ioffe, Ann. Phys. (Amsterdam) **375**, 378 (2016).
[27] J. Kurchan, J. Stat. Phys. **171**, 965 (2018).
[28] C. Cichowlas, P. Bonaïti, F. Debbasch, and M. Brachet, Phys. Rev. Lett. **95**, 264502 (2005).
[29] G. Krstulovic and M. E. Brachet, Physica (Amsterdam) **237D**, 2015 (2008).
[30] S. S. Ray, U. Frisch, S. Nazarenko, and T. Matsumoto, Phys. Rev. E **84**, 016301 (2011).
[31] A. J. Majda and I. Timofeyev, Proc. Natl. Acad. Sci. U.S.A. **97**, 12413 (2000).
[32] See Supplemental Material at http://link.aps.org/supplemental/10.1103/PhysRevLett.127.124501 for details on thermalized fluids, technical details of the numerical

simulations, the complete derivation of our linearized theory of decorrelators in one and three dimensions, including its thermal bound, spatial spread, and saturation and associated figures, a movie of time evolution of how a perturbation spreads in a 3D thermalized fluid, and additional Refs. [33–38].

[33] U. Frisch and J. Bec, in *New Trends in Turbulence Turbulence: Nouveaux Aspects*, edited by M. Lesieur, A. Yaglom, and F. David, Les Houches - Ecole d'Ete de Physique Theorique Vol. 74 (Springer, Berlin, Heidelberg, 2001), pp. 341–383, https://doi.org/10.1007/3-540-45674-0_7.

[34] J. Bec and K. Khanin, Phys. Rep. **447**, 1 (2007).

[35] S. S. Ray, Pramana **84**, 395 (2015).

[36] D. Venkataraman and S. S. Ray, Proc. R. Soc. A **473**, 20160585 (2017).

[37] P. Clark Di Leoni, P. D. Mininni, and M. E. Brachet, Phys. Rev. Fluids **3**, 014603 (2018).

[38] S. D. Murugan, U. Frisch, S. Nazarenko, N. Besse, and S. S. Ray, Phys. Rev. Research **2**, 033202 (2020).

[39] W. T. Ashurst, A. R. Kerstein, R. M. Kerr, and C. H. Gibson, Phys. Fluids **30**, 2343 (1987).

[40] B. Galanti, J. D. Gibbon, and M. Heritage, Nonlinearity **10**, 1675 (1997).

[41] T. Scaffidi and E. Altman, Phys. Rev. B **100**, 155128 (2019).